World Journal of Radiology

Online Submissions: http://www.wjgnet.com/1949-8470office
wjr@wjgnet.com
doi:10.4329/wjr.v1.i1.72

*World J Radiol* 2009 December 31; 1(1): 72-85
ISSN 1949-8470 (online)


REVIEW

# Magnetic resonance imaging of the liver: New imaging strategies for evaluating focal liver lesions

Kenneth Coenegrachts

Kenneth Coenegrachts, Department of Radiology, AZ St.-Jan Brugge-Oostende AV, Ruddershove 10, B-8000 Bruges, Belgium
Author contributions: Coenegrachts K contributed solely to this paper.
Correspondence to: Kenneth Coenegrachts, MD, PhD, Department of Radiology, AZ St.-Jan Brugge-Oostende AV, Ruddershove 10, B-8000 Bruges, Belgium. kenneth.coenegrachts@azbrugge.be
Telephone: +32-50-452103 Fax: +32-50-452146
Received: October 10, 2009 Revised: November 12, 2009
Accepted: November 16, 2009
Published online: December 31, 2009

## Abstract

The early detection of focal liver lesions, particularly those which are malignant, is of utmost importance. The resection of liver metastases of some malignancies (including colorectal cancer) has been shown to improve the survival of patients. Exact knowledge of the number, size, and regional distribution of liver metastases is essential to determine their resectability. Almost all focal liver lesions larger than 10 mm are demonstrated with current imaging techniques but the detection of smaller focal liver lesions is still relatively poor. One of the advantages of magnetic resonance imaging (MRI) of the liver is better soft tissue contrast (compared to other radiologic modalities), which allows better detection and characterization of the focal liver lesions in question. Developments in MRI hardware and software and the availability of novel MRI contrast agents have further improved the diagnostic yield of MRI in lesion detection and characterization. Although the primary modalities for liver imaging are ultrasound and computed tomography, recent studies have suggested that MRI is the most sensitive method for detecting small liver metastatic lesions, and MRI is now considered the pre-operative standard method for diagnosis. Two recent developments in MRI sequences for the upper abdomen comprise unenhanced diffusion-weighted imaging (DWI), and keyhole-based dynamic contrast-enhanced (DCE) MRI (4D THRIVE). DWI allows improved detection (b = 10 s/mm$^2$) of small (< 10 mm) focal liver lesions in particular, and is useful as a road map sequence. Also, using higher b-values, the calculation of the apparent diffusion coefficient value, true diffusion coefficient, D, and the perfusion fraction, f, has been used for the characterization of focal liver lesions. DCE 4D THRIVE enables MRI of the liver with high temporal and spatial resolution and full liver coverage. 4D THRIVE improves evaluation of focal liver lesions, providing multiple arterial and venous phases, and allows the calculation of perfusion parameters using pharmacokinetic models. 4D THRIVE has potential benefits in terms of detection, characterization and staging of focal liver lesions and in monitoring therapy.



**Key words:** Magnetic resonance imaging; Liver neoplasms; Diffusion-weighted magnetic resonance imaging; 4D THRIVE; Dynamic contrast-enhanced magnetic resonance imaging; Contrast agents

**Peer reviewer:** Hui-Xiong Xu, MD, PhD, Professor, Department of Medical Ultrasonics, Institute of Diagnostic and Interventional Ultrasound, Sun Yat-Sen University, 58 Zhongshan Road 2, Guangzhou 510080, Guangdong Province, China

Coenegrachts K. Magnetic resonance imaging of the liver: New imaging strategies for evaluating focal liver lesions. *World J Radiol* 2009; 1(1): 72-85 Available from: URL: http://www.wjgnet.com/1949-8470/full/v1/i1/72.htm DOI: http://dx.doi.org/10.4329/wjr.v1.i1.72

## INTRODUCTION

The early detection of focal liver lesions, particularly those which are malignant, is of utmost importance. For

example, the resection of liver metastases of some malignancies, including colorectal cancer, has been shown to improve the survival of patients[1]. Exact knowledge of the number, size, and regional distribution of liver metastases is essential to determine their resectability. Almost all focal liver lesions larger than 10 mm can be demonstrated with current imaging techniques but the detection of smaller focal liver lesions is still relatively poor[2-6]. Transabdominal ultrasonography (US) is widely used to assess the liver, but has some limitations: it needs considerable operator expertise and often reveals equivocal results in patients with chemotherapy-induced fatty infiltration of the liver[7]. Contrast-enhanced (CE)-US has increased the potential for characterization of malignant and benign focal liver lesions compared with baseline US. CE-US increased diagnostic confidence in the detection and characterization of liver metastases compared with standard US[8]. Limitations of CE-US are essentially the same as those of US and are related to the presence of bowel gas and to the patient's body habitus[9]. Among radiologic imaging techniques, US and CE-US are relatively inexpensive and therefore are used in many general radiology departments[10,11]. However, for accurate oncologic staging, US examinations often require to be complemented by other imaging techniques.

Diagnostically problematic cases using US are often referred for a computed tomography (CT) or magnetic resonance imaging (MRI) examination. With the introduction of multi-slice CT (MSCT) imaging, the use of MSCT in oncologic patients to search for lung, liver, and lymph node metastases in the body has substantially increased[12,13]. The development of MSCT has substantially increased patient throughput allowing volume coverage of the whole thorax and abdomen in one breath-hold. However, even using MSCT, the sensitivity and ability to discriminate between small liver metastases and other small focal liver lesions is inferior compared to MRI[12].

Combined positron emission tomography (PET)/CT images have significant advantages over either technique alone because it provides both functional and anatomical data. The most significant additional information provided by PET/CT relates to the accurate detection of distant metastases. In a study by Wiering *et al*[14], FDG-PET was clearly superior to CT in predicting extrahepatic disease in patients with colorectal liver metastases.

One of the advantages of MRI in liver imaging is the better soft tissue contrast, which reveals better characterization of focal liver lesions in question. The development of liver-specific MRI contrast agents has further improved the diagnostic yield of MRI in lesion detection and characterization[15,16]. Although the primary modalities for liver imaging are US and CT, recent studies have suggested that CE-MRI is the most sensitive method for detecting small liver metastases and MRI is now considered the pre-operative standard[17-21]. Developments in MRI hardware and software and the availability of novel MRI contrast agents have improved small focal liver lesion detection[22]. During the last few years, MRI enhanced with superparamagnetic iron oxide (SPIO) probably has been considered the most sensitive method for detecting so-called hypovascular liver metastases[22]. In the few studies which have compared different liver-specific agents, SPIO-enhanced MRI has demonstrated varying degrees of superiority, particularly for small focal liver lesions[23,24]. Furthermore, the importance of using ferucarbotran (SPIO contrast agent) by bolus injection, providing the opportunity to obtain dynamic T1-weighted (T1w) images has been described[22]. Ward[22] has found early T1-enhancement on 3D fat-suppressed T1w gradient echo (GE) images to be particularly valuable for depicting small focal liver lesions. The T1-effect is considerably less than occurs with extracellular fluid gadolinium (Gd)-based contrast agents but this is often beneficial in the context of metastatic disease. Liver and vessels often have a similar signal intensity that produces a virtual blank canvas against which small liver metastases are extremely conspicuous and reliably distinguished from vessels. The combination of thin-slice 3D T1w and T2w imaging after SPIO increases diagnostic confidence and is more accurate for small focal liver lesion detection than delayed T2w imaging alone[22].

## NEW DEVELOPMENTS IN MRI SEQUENCES FOR THE LIVER

### *Diffusion-weighted imaging (DWI) [Single-shot spin-echo echo-planar imaging (SS SE-EPI sequence)]*

Diffusion-weighted MRI is sensitive to molecular diffusion as a result of random and microscopic translational motion of molecules, known as Brownian motion. Random motion in the field gradient produces incoherent phase shifts that results in signal attenuation. Flowing spins induce the same attenuation effect; the pseudorandom organization of the moving spins at the voxel level, such as perfusion, can also be considered to be an incoherent motion, and this effect can induce much larger signal attenuation than the diffusion effect on an image with very low motion-probing gradients (MPGs)[25,26]. The strength of the applied MPG increases with increasing b-value (expressed in s/mm$^2$). On the basis of this theory, the apparent diffusion coefficient (ADC) value calculated from the images with no and low MPGs ($ADC_{low}$) is considered to be more strongly influenced by the flowing spins (microcirculation) than molecular diffusion. The true diffusion coefficient, D, can be obtained from the calculation from images with the higher b-values[25,26]. D as measured at intravoxel incoherent motion (IVIM) MRI is a true parameter of molecular diffusion[25,26]. It therefore permits characterization of tissues and pathologic conditions. Furthermore, the perfusion fraction, f, as measured at IVIM MRI is the (microperfusion) deviation factor representing the fractional

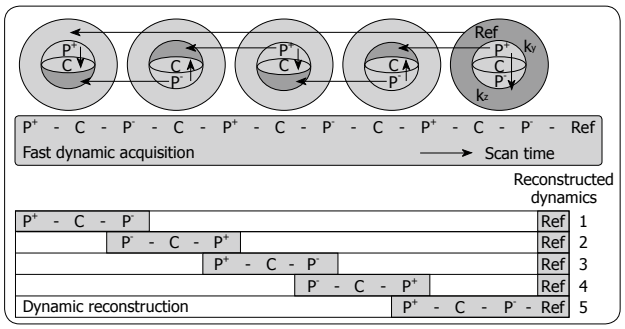


**Figure 1 Schematic depiction of the alternating viewsharing technique.** The central ky-kz disk defined by the keyhole percentage is subdivided in 3 regions, $P^+$, C and $P^-$, where $P^+$ and $P^-$ cover positive and negative peripheral regions in this central disk and C is the central region as shown. The central region C is acquired in each dynamic scan while regions $P^+$ and $P^-$ are shared with subsequent dynamic scans according to an alternating viewsharing scheme: $P^+$-C-$P^-$-C-$P^+$-C-$P^-$-C-$P^+$-Ref. The $P^-$ and $P^+$ parts from subsequent keyhole scans are shared in the reconstruction process.

volume (of spins) occupied in the voxel by flowing spins (= sum of the spins in the microcirculation and spins in turbulent flow)[27].

During recent years, DWI of the liver, using echo planar imaging sequences with low b-values, has been proven to be useful for the detection of focal liver lesions because of the black-blood effect when using low b-values. The black-blood effect renders blood vessels black while focal liver lesions remain bright. The use of the black-blood effect for facilitating detection of focal liver lesions, by better differentiation between small vascular branches and small focal liver lesions, has been described previously[28]. This black-blood effect has proven to be useful in detecting focal liver lesions especially those smaller than 10 mm)[29-32]. Respiratory-triggered SS SE-EPI is preferred for liver MRI as respiratory-triggering increases the signal-to-noise ratio (SNR) and helps to avoid false-negative results but also false-positive results due to noise. In our experience[29], for focal liver lesion detection a b-value of b = 10 s/mm$^2$ is to be preferred over b = 20 or 50 s/mm$^2$.

DWI of the liver, using SS SE-EPI with low and high b-values, seems promising for the characterization of focal liver lesions by calculating D, f and $ADC_{low}$[25-27,33,34].

The SS SE-EPI sequence is prone to artifacts (e.g. air from the bowel loops). Therefore, we recommend giving each patient 0.5 L of tap water just before the start of each MRI examination. We also recommend starting each MRI examination of the upper abdomen with the SS SE-EPI sequence, using respiratory-triggering to optimize the SNR. The SS SE-EPI sequence can then be used as a road map sequence to guide the rest of the MRI examination.

### *T1w dynamic contrast-enhanced (DCE) MRI (4D THRIVE)*

Three-phased DCE MRI is currently accepted as an important imaging tool for detecting and characterizing tumors in abdominal organs such as the liver[35]. The hepatic purely arterial phase is especially important to distinguish fast enhancing lesions from slow contrast uptake in liver parenchyma[36-38]. Also, imaging of the portal venous phase is crucial for characterizing focal liver lesions. However, often the arterial hepatic phase will overlap with enhancement of blood coming from the portal vein during the 20-s acquisition time typically achieved in 3-phased MRI[38]. To address this problem, Beck *et al*[39] recently proposed a fast imaging technique called CENTRA Plus or 4D THRIVE, combining the principles of keyhole imaging with half-Fourier acquisition to achieve a higher temporal resolution with full liver coverage and a minor decrease of the spatial resolution. The elliptical centric keyhole method consists of dynamically acquiring a limited number of central ky-kz-space profiles (disk), and sharing the high spatial resolution information from a single full data set called reference (Figure 1). To further accelerate the technique, an alternating view-sharing technique, as described in references 40 and 41, was applied. With this strategy it was shown that the precision of contrast-enhancement sampling could be improved[39].

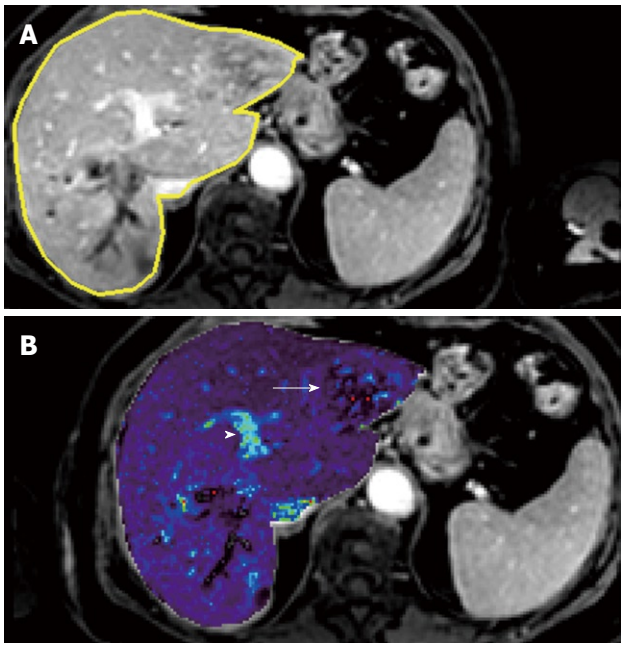


**Figure 2 Liver metastasis in a 68-year-old woman using transverse contrast-enhanced 4D THRIVE.** The reference image using 4D THRIVE in the delayed phase (A) is shown with corresponding automatically calculated Kep map (B). The parametric map shows the liver metastasis (white arrow) as a heterogeneous lesion with ring enhancement. The portal vein is indicated by the white arrowhead.

DCE MRI sequences (4D THRIVE) with higher temporal resolution can also be used to generate parametric maps (Figure 2) and to compute perfusion and permeability parameters using pharmacokinetic models, with potential benefits in terms of detection, characterization and staging of tumors and in monitoring therapy[42,43]. To date, reports of liver perfusion at MRI are limited in number and vary considerably[44]. T1w dynamic CE-MRI seems a promising method for the detection of cancer[45]. Remarkably, encouraging results

have been obtained despite considerable variation in both the methods of data acquisition and analysis (e.g. visual inspection[46], parametric analysis[47], pharmacokinetic[48] or physiologic[49] modeling). In most cases, only one to a few slices within the whole liver parenchyma have been used to evaluate perfusion parameters.

As a result of new developments in MRI scanning technologies, it is now possible to perform T1w CE-MRI of the entire liver with high spatial and temporal resolution, using the above mentioned T1w DCE 4D THRIVE sequence. This 4D THRIVE sequence has already been evaluated for its ability to differentiate benign from malignant focal liver lesions[41].

## MRI CHARACTERISTICS OF DIFFERENT FOCAL LIVER LESIONS

### *Hepatic cysts*

Hepatic cysts, including those without further pathologic importance, almost always can be accurately diagnosed using US. Only rarely are additional imaging sequences needed; non-complicated hepatic cysts can be easily characterized using MRI.

Complex cystic focal liver lesions are lesions containing large fluid-filled areas. They are increasingly commonly found in clinical practice as a result of the increased use of hepatic imaging. Complex cystic focal liver lesions represent a wide spectrum of lesions that include both benign and malignant lesions[50]. The most frequently encountered complex cystic focal liver lesions comprise hepatic cysts complicated by intracystic hemorrhage, abscesses (see description below), hematomas, cystadenomas and cystadenocarcinomas.

Hepatic cysts complicated with acute hemorrhage and acute hematomas are typically hyperintense on unenhanced T1w imaging. The differentiation between cystadenomas and cystadenocarcinomas using only imaging criteria can be very difficult and so-called borderline lesions are frequently encountered. The probability of underlying malignancy in general increases with increased thickening of the septations, increased septal calcifications and increased presence of mural thickening. Using contrast-enhanced MRI, complete non-enhancement using dynamic MRI or slow contrast-enhancement of the septations and mural nodules in the arterial phase and persistent contrast-enhancement in the portal and late venous phases most frequently are exhibited in benign complex cystic focal liver lesions. In contrast, hypo-enhancement in the late venous phases most frequently is seen in malignant complex cystic focal liver lesions[50].

### *Liver hemangiomas*

Liver hemangiomas are the most common benign tumors of the liver, with a reported incidence ranging from 1% to 20%. Hemangiomas occur more commonly in women (female/male ratio 5:1). A hemangioma usually is well circumscribed and blood filled. Hemangiomas larger than 10 cm are designated as giant hemangiomas[51].

On cut sections, hemangiomas almost always are inhomogeneous, with areas of fibrosis, necrosis, and cystic change. Sometimes abundant fibrous tissue completely replaces the lesion. Calcification is rare in this tumor (less than 10%) and can be either large and coarse, with phlebolith-like thrombi within the vascular channels of the hemangioma[52,53]. Microscopically it is composed of multiple vascular channels lined by a single layer of endothelial cells supported by a thin fibrous stroma.

On MRI, hemangiomas characteristically demonstrate marked hyperintensity on T2w images, which may contain low-intensity areas that correlate with zones of fibrosis[54]. In the characterization of hemangiomas, the comparison of T2w images with short echo time (TE) and long TE is important. In most cases, hemangiomas are still displayed as relatively hyperintense, compared with the surrounding liver parenchyma, on long TE T2w images and the contours and volume of the displayed hemangioma are exactly comparable on short TE and long TE T2w imaging. This finding can also be seen in hypervascular liver metastases. Further differentiation of hemangiomas and so-called hypervascular liver metastases is described below.

On unenhanced T1w images, a hemangioma displays most commonly as a well-defined slightly hypo-intense tumor with lobulated borders. The pattern of peripheral "nodular" enhancement after Gd injection was seen as highly specific for hemangioma compared with rim enhancement noted in metastases[54,55].

Three enhancement patterns of hemangioma with Gd-enhanced GE imaging have been noted:

**Immediate and complete enhancement of small lesions (so-called capillary hemangiomas):** Capillary hemangiomas are rapidly filling hemangiomas that occur significantly more often in small hemangiomas (42% of hemangiomas are less than 1 cm in diameter)[56]. On CT and MRI, capillary hemangiomas show immediate homogenous contrast-enhancement in the arterial phase; thus, differentiation from other hypervascular tumors is difficult. According to various authors, up to 83% of the smaller hemangiomas (less than 3 cm) showed iso-attenuation compared with the arterial system in all 3 phases of enhanced scanning[57,58]. During the portal venous phase of contrast-enhancement, capillary hemangiomas show an attenuation equivalent to that of the aorta. In the delayed phase, on CT or MRI, hemangiomas remain hyperattenuating or hyperintense, whereas hypervascular metastases do not[52].

During the perfusion phase using SPIO-enhanced T1w GE imaging, and persisting during delayed imaging, a significant increase in signal intensity has been reported on T1w GE imaging as a result of pooling of SPIO in the vascular spaces of a hemangioma[59-61]. This pooling of SPIO also explains that hemangiomas often lose signal on delayed T2w imaging[59].

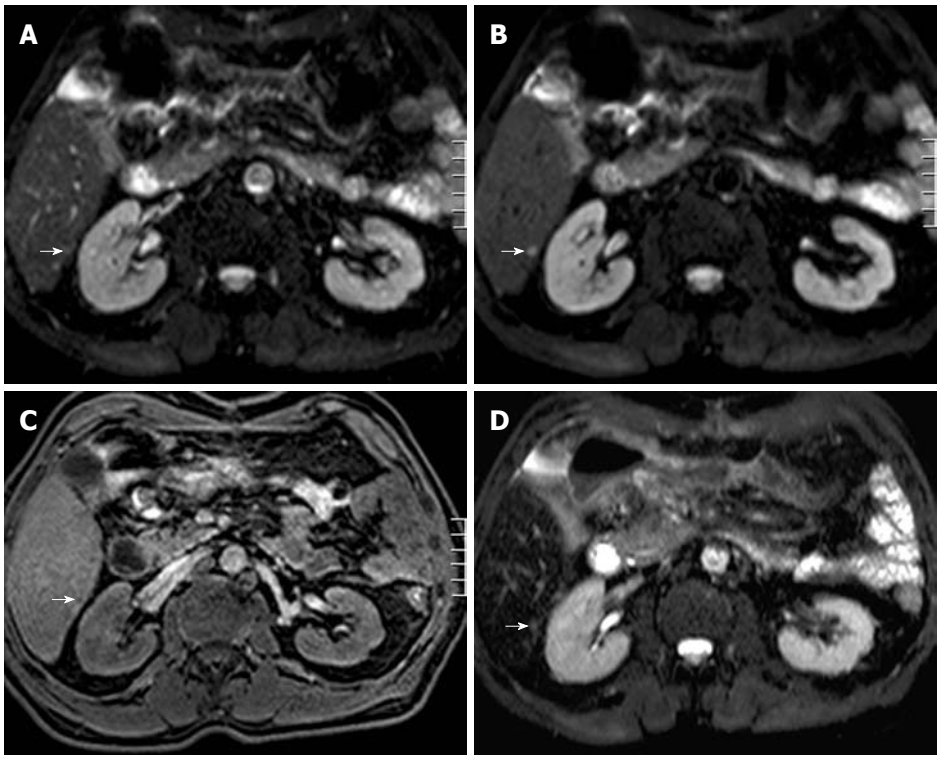


**Figure 3 Transverse single-shot spin-echo echo-planar imaging (SS SE-EPI), fat-suppressed T1w 3D GE and SPIO-enhanced T2w TSE (short TE with fat suppression) image in a 62-year-old man.** A: A transverse SS SE-EPI image using b = 0 s/mm$^2$ in a 62-year-old man barely detecting any visible lesion in the area indicated by the white arrow; B: A transverse SS SE-EPI image using b = 10 s/mm$^2$ in the 62-year-old man clearly detecting the liver metastasis (white arrow); C: A transverse fat-suppressed T1w 3D GE image in the portal-venous phase after intravenous injection of SPIO in the 62-year-old man barely detecting the liver metastasis (white arrow); D: A transverse SPIO-enhanced T2w TSE (short TE with fat suppression) image in the 62-year-old man barely detecting the liver metastasis (white arrow). SS SE-EPI: Single-shot spin-echo echo-planar imaging; GE: Gradient echo; T1w: T1-weighted; SPIO: Superparamagnetic iron oxide; TE: Echo time.

**Peripheral nodular enhancement progressing centripetally to uniform enhancement and peripheral nodular enhancement with persistent central hypointensity[62]:** These 2 last findings are more frequently depicted in larger (cavernous) hemangiomas. Uniform enhancement throughout the lesion on delayed images should not be used as a criterion for diagnosis because this will only lower the specificity[63]. In the majority of cases, the combination of T2w and serial dynamic Gd images allows a confident diagnosis of hemangiomas[54]. On the delayed liver-specific phase, after Gd-BOPTA (gadobenate dimeglumine), hemangiomas tend to be hypo-intense compared with the surrounding liver parenchyma[64,65].

### *"Hypovascular" liver metastases*

Among solid hypovascular liver lesions, metastases constitute the main group. Hepatic metastases are the most frequent malignancies in the liver. The incidence of hepatic metastases is approximately 40% in patients with colorectal cancer[66]. In the United States, approximately 50 000 cases of hepatic colorectal metastases are seen annually[67]. Lesion detection is size related. When reviewing the literature, a lower threshold for detection is about 1 cm[68]. Unfortunately, postmortem assessment of the size of liver metastases has shown that the ratio between metastases larger than 1 cm and those smaller than 1 cm is approximately 1:1.6 for metastases of colorectal adenocarcinoma and 1:4 for other liver metastases[69]. This clearly indicates that a capacity to accurately detect and characterize metastases smaller than 1 cm is necessary.

Detection and characterization of small (< 1 cm) focal liver lesions using MDCT is inferior to MRI[12]. Furthermore, with the use of the respiratory-triggered SS SE-EPI sequence, detection of focal liver lesions even down to 3 mm is possible using MRI[29]. In a study by Coenegrachts *et al*[29], unenhanced respiratory-triggered SS SE-EPI performed better than SPIO-enhanced MRI (literature gold standard[22]) for detecting so-called hypovascular liver metastases (Figure 3A-D). Therefore, the SS SE-EPI sequence is ideally suited to be used as the first sequence (road map sequence) during an MRI examination of the liver. In most cases, the respiratory-triggered SS SE-EPI depicts the whole liver with good image quality and excellent contrast-to-noise ratio (CNR). In that case, if no focal liver lesions can be detected using the unenhanced respiratory-triggered SS SE-EPI sequence, then the presence of malignant focal liver lesions is extremely unlikely (high negative predictive value of SS SE-EPI). The signal intensity of the metastases is moderately increased compared with the surrounding hepatic tissue on T2w images and decreased on unenhanced T1w images[70]. Malignant tumors tend to have margins that are not sharply defined.

Liquefactive necrosis within the metastasis increases signal intensity on T2w images, whereas coagulative necrosis[71], desmoplastic reaction, or calcifications[72] decrease signal intensity on T2w images.

In some cases, the production of paramagnetic substances modifies the appearance of metastases on T1w images. The melanin present in the metastases from melanoma increases the signal intensity on T1w images. The presence of mucin within metastases can also increase the signal intensity on T1w images[73]. On T1w DCE imaging, in the arterial phase "hypovascular" liver metastases can show a fleeting ring enhancement

that blurs the margins of the lesions and corresponds to a desmoplastic reaction, inflammatory infiltration, and vascular proliferation in the tumor-liver parenchyma margin[74]. Enhancement progresses centrally with concomitant peripheral wash-out[74]. In the venous phase, liver metastases are hypo-intense compared with the surrounding liver parenchyma.

During the perfusion phase using SPIO-enhanced T1w GE imaging, ring enhancement is highly suggestive of malignant liver lesions[61]. Metastases do not contain reticulo-endothelial system cells; thus, after SPIO injection the liver metastasis CNR is improved with increased lesion conspicuity and detection compared with unenhanced T2w images[14,19,75].

In clinical practice, the differentiation between small (< 10 mm), so-called fibrous, liver hemangiomas and hypovascular liver metastases is a frequent problem. For the differentiation of focal liver lesions, the calculation of D, f and $ADC_{low}$ seems promising in reducing liver biopsy procedures in the future. However, for the characterization of small liver hemangiomas and small liver metastases[27], more research is needed. Nonetheless, if an operation is planned, the surgeon has an accurate means of guidance during the operation using intra-operative ultrasound to further characterize these small focal liver lesions in those areas where a focal liver lesion is detected with the SS SE-EPI sequence. This allows the surgeon to locally treat small malignant focal liver lesions with minimally-invasive techniques. This should likely benefit the patients' prognosis by optimizing the removal of all malignant deposits within the liver during one treatment session.

### *"Hypervascular" liver metastases*

Hypervascular metastases are those with an abundant blood supply, typically greater than that of normal liver. These tumors include choriocarcinoma, renal cell carcinoma, thyroid carcinoma, breast carcinoma, melanoma, carcinoid tumor, and islet cell tumor. In general, these tumors may show a hyperintense signal on T2w images, and so potentially could be mistaken for a hemangioma[76]. In addition, most of these tumors have an increased tendency to have an intratumoral hemorrhage. This results in increased signal on unenhanced T1w images as well as T2w images. Melanoma, as a result of the T1 shortening effect of melanin, shows an increased signal on the T1w image even if hemorrhage is not present.

Hypervascular liver metastases show significant enhancement during the arterial phase of ECF agent contrast-enhancement, which is the most important phase for lesion detection, whereas hypovascular metastases are best imaged during the portal venous phase. Detection of smaller hypervascular liver metastases in particular is enhanced with the use of 4D THRIVE - obtaining multiple arterial phases of the whole liver in high spatial resolution - thereby also optimizing the timing of imaging in the appropriate arterial time window for visualizing the sometimes very short arterial hyperenhancing lesions.

In the portal venous phase, hypervascular metastases usually show rapid wash-out, which renders them hypo-intense compared with the surrounding liver parenchyma.

On delayed phase, the ECF accumulates in the center of larger (hypovascular and hypervascular) liver metastases because of its pooling in the extracellular fibrotic component of the lesion, thus becoming progressively hyperintense to the surrounding liver parenchyma (delayed central pooling).

The appearance of a solitary hypervascular liver metastasis and a solitary hepatocellular carcinoma (HCC) can be comparable in some cases. However, differentiation often is facilitated as HCC is almost always encountered in a cirrhotic liver parenchyma whereas a hypervascular liver metastasis is encountered in a "normal" liver parenchyma. Further, specific morphologic criteria can aid in the differentiation of both focal liver lesions (see description in the sections on "hypervascular" liver metastases and HCC).

### *Focal nodular hyperplasia (FNH)*

FNH is a benign tumor-like lesion that results from a hyperplastic rather than a neoplastic process[77]. This explains the nearly iso-intense and homogeneous appearance of FNH with the surrounding liver parenchyma on imaging. When present, the central scar presents as hyperintense on T2w imaging and hypo-intense on unenhanced T1w imaging. In the absence of a central scar, an FNH can hardly be detected using unenhanced imaging. Dynamic Gd-based CE MRI shows a marked enhancement in the arterial phase of the lesion, which persists as slightly hyperintense or iso-intense in the portal venous and distribution phase, whereas the central scar appears hypo-intense in the arterial and portal venous phase to become hyperintense in the distribution phase[74,78]. For detecting smaller FNHs in particular, the use of 4D THRIVE - obtaining multiple arterial phases of the whole liver in high spatial resolution - enhances the visualization of FNHs sometimes showing only very short arterial hyperenhancement.

MRI contrast agents with liver-specific properties are helpful in characterizing FNH. In FNH, there is prolonged and excessive hepatocellular accumulation of hepatocyte-specific contrast agent because of the structural alteration of the biliary canalicular system that does not communicate with or derive from the surrounding normal hepatic biliary system. Two or three hours after IV injection of Gd-BOPTA, typical cases FNHs are hyperintense (to iso-intense) compared with the surrounding liver parenchyma. This behavior is distinct from that seen in adenomas, which do not show significant enhancement compared to the liver parenchyma during the delayed phase[79].

However, accurate characterization of FNH is not always possible because atypical features can confound

the interpretation. While the absence of a scar in small FNHs cannot be considered atypical, it does make it more difficult to distinguish FNH from other hypervascular tumors. Again, delayed phase imaging proved useful in a study by Grazioli *et al*[79]; all 49 small FNHs showed either hyperintense [33 (67%) lesions] or isointense [16 (33%) lesions] enhancement. In addition, a central scar was detected on delayed images in 15 (31%) of the 49 lesions compared with only 7 (14%) of 49 on dynamic phase images. Anecdotal experience by Grazioli *et al*[79] with 4 cases of adenoma and one of adenomatosis (unpublished data) demonstrated a markedly hypointense appearance on delayed images relative to FNH or normal liver. Although adenomas have functioning hepatocytes, they lack bile ducts. It is therefore likely that bilirubin metabolism is blocked in the adenoma, as confirmed by the absence of bile in resected adenomas[80]. Altered hepatocellular metabolism may inhibit the uptake of Gd-BOPTA in the adenoma thereby accounting for its hypo-intense appearance on delayed MRI images. Radionuclide imaging with sulfur colloid is generally considered useful in the characterization of FNH because of the uptake of tracer by the Kupffer cells. However, uptake is seen in only approximately two-thirds of lesions[81] and is limited to the detection only of large lesions.

Kupffer cells usually are observed within FNH and are a major histologic feature of this lesion. Uptake of SPIO by FNH is common, with the lesions showing significant decreases in signal intensity on ferumoxides-enhanced T2w images[82]. Signal drop reflects the presence of Kupffer cells within the lesion. Nevertheless, the amount and distribution of Kupffer cells within the nodule can vary and yield different patterns of signal decrease: some small FNHs (less than 3 cm) show homogenous signal drop similar to that observed in the surrounding parenchyma, whereas large FNHs may show inhomogeneous signal drop. The central scar excludes iron particles and is readily demonstrated as a hyperintense central stellate area. That finding corresponds to the high signal area seen on T2w unenhanced images but higher conspicuity generally is found after the use of SPIO agents[83]. Furthermore, adenomas have also been reported to demonstrate signal drop after SPIO administration using T2w imaging[60].

### Telangiectatic FNH

Telangiectatic FNH is an uncommon hepatic neoplasm that demonstrates histologic and imaging features that are different from those of typical FNH[84]. A common finding of telangiectatic FNH in the study of Attal *et al*[84] was strong arterial enhancement, which is also seen in most cases of typical FNH[85]. However, additional imaging characteristics of telangiectatic FNH are described in the literature: (1) A heterogeneous pattern is a very rare feature in FNH and was observed in 2.4% of the cases in a radiologic-pathologic study by Vilgrain *et al*[86]. The main causes of heterogeneity in the study of Attal *et al*[84] were necrosis, the degree of sinusoidal dilatation, and the presence of hemorrhagic foci. Hemorrhage, an unusual finding in FNH, was more commonly observed in larger lesions; (2) Hyperintensity on T1w MRI images is very rare in FNH and was observed in 2.1%-6.0% of cases in previous studies[86,87]. It is well known that hyperintensity on T1w MRI images may be to the result of different pathologic changes, including fat deposition, copper accumulation, high protein concentrations, blood degradation products, or sinusoidal dilatation[88]; (3) Strong hyperintensity on T2w MRI images is also a rare finding in FNH; (4) A central scar was rarely present in the study by Attal *et al*[84]; and (5) Persistent lesion enhancement on delayed phase images was a frequent feature observed by Attal *et al*[84]. This finding has been described only once in FNH, to our knowledge[89]. Persistent contrast agent uptake in telangiectatic FNH could be related to sinusoidal dilatation.

Attal *et al*[84] concluded that telangiectatic FNH is an uncommon entity that differs from typical FNH at imaging. Lesions are multiple in 62% of cases. Atypical features of FNH often observed with telangiectatic FNH are lack of a central scar, lesion heterogeneity, hyperintensity on T1w MRI images, strong hyperintensity on T2w MRI images, and persistent contrast-enhancement on delayed phase T1w MRI images.

### Hepatic adenoma

DCE MRI, whether performed with ECF agents or liver targeted agents, can demonstrate early arterial enhancement that becomes iso-intense or hypo-intense in the portal venous phase, although this usually is less marked than in cases of FNH. In cases of previous hemorrhage, the arterial enhancement can be inhomogenous[74]. On Gd-enhanced MRI, most adenomas are hyperintense on arterial and early portal venous phase images, whereas on late portal venous phase images and equilibrium phase images most appear iso-intense overall. For detecting smaller adenomas in particular, the use of 4D THRIVE - obtaining multiple arterial phases of the whole liver in high spatial resolution - also enhances the visualization of adenomas sometimes showing only very short arterial hyperenhancement.

On delayed phase images after injection of Gd-BOPTA, most lesions appear hypo-intense, indicating a lack of uptake by the lesions (see also above; description of FNH)[74]. Therefore, delayed phase imaging using hepatocyte-specific contrast agents can be useful in the differentiation of adenomas and FNHs. Kupffer cells often are found in hepatic adenoma but in reduced numbers and with little or no function, as reflected by the absent or diminished uptake of technetium-99m sulfur colloid[90]. Hepatic adenomas usually do not show uptake of SPIO particles, resulting in increased tumor-liver CNR on T2w images. However, occasionally hepatic adenomas have shown some degree of uptake[82],

with an inhomogeneous signal drop whose entity usually is less than in FNH. Uptake of SPIO in hepatic adenoma appears to be to the result of pooling of the contrast agent within the peliosis-like dilated vessels that characterize them[60]. However, in several cases, no significant difference of signal loss was observed between FNH and hepatic adenoma[83].

### HCC

HCC is the most frequent primary tumor of the liver (80%-90%) and represents more than 5% of all cancers, with an incidence of more than 500 000 new cases per year throughout the world[91]. Its incidence in developing countries is 2-3 times higher than in developed countries, although its incidence is rising in Western countries and in Japan[92]. The most significant risk factor, regardless of etiology, is the presence of liver cirrhosis[93], particularly when secondary to viral infection and high alcohol intake. Other risk factors include hemochromatosis and primary biliary cirrhosis[91].

Pathologically, HCC develops *de novo* or most frequently develops in a multistep fashion in the following sequence: from low-grade dysplastic nodule (LGDN), to high-grade dysplastic nodule (HGDN), early HCC, well-differentiated HCC, and finally to a moderately differentiated HCC. Differentiation between early HCC and DN is a very important issue in the clinical setting. CT during arterial portography (CTAP) is the most sensitive tool in the differentiation of premalignant/borderline lesions (LGDN and HGDN) and early HCC[94].

The formation of a pseudocapsule around the lesion (constructed usually from connective fibrous tissue) and of a septum within the tumor is frequently observed with the development of HCC. This may derive from an interaction between the tumor and host liver and may interfere with the growth and invasion of the HCC[95].

On T2w images, most HCCs demonstrate increased signal compared to the surrounding liver, although the tumors tend to be inhomogeneous[96]. The T1 appearance of HCC ranges from hypo-intense to slightly hyperintense, depending on fat content, copper deposition within the tumor, and the degree of differentiation[96].

Several studies have shown that the characteristic HCC profile includes an intense arterial uptake but is followed by contrast agent wash-out in the delayed venous phase[97]. The recognition of the diagnostic value of contrast agent wash-out allowed the refinement of the criteria as reflected in the recent American Association for the Study of Liver Diseases guidelines and in the unpublished consensus of the European Association for the Study of the Liver experts that met in 2005[97].

Dynamic T1w imaging during the arterial phase is of utmost importance for the detection of small (< 10 mm) HCCs, because they may be occult at other pulse sequences and on portal venous and equilibrium phase images[98]. Also, the use of 4D THRIVE (multiple arterial phase imaging) enhances the detection of smaller HCCs in particular.

In these cases, the T1w and T2w appearance of the tumors may not be substantially different from that of the surrounding liver, or the underlying liver heterogeneity may make the tumor difficult to detect[96]. DWI improves the detection of HCCs in particular, and the differentiation of pseudotumoral lesions compared with conventional MRI in liver cirrhosis[99].

Controversies regarding the optimal timing to capture the arterial phase exist[100-102], but as discussed this problem can be solved using 4D THRIVE.

Dysplastic nodules are defined as spontaneously hyperintense on T1w images without (intense) contrast-enhancement in the arterial phase during DCE imaging[97]. However, the differentiation between dysplastic nodules, especially HGDN, and early HCC can often be difficult[94], as early HCC often can have a different appearance on T1w and T2w imaging compared with overt HCC[94]. The most sensitive modality capable of clearly depicting the early carcinogenesis process is CTAP. However, many, well-differentiated, early HCCs appear as hypovascular nodules on CTAP. In cases where portal blood is reduced, but arterial blood flow has not yet increased, both HGDNs as well as early HCCs are depicted as sharply delineated hypo-enhancing nodules compared with the surrounding liver parenchyma[94]. In those cases, differentiation between HGDNs and early HCCs is impossible on imaging.

With SPIO particles, HCCs generally do not show a significant decrease in signal intensity, although signal intensity loss was seen in some individual HCCs[82]. The signal intensity of the normal liver does decrease, however, thereby improving the CNR of malignant focal liver lesions. According to Lim *et al*[103], HCC conspicuity after SPIO depends on differences in the number of Kupffer cells between the lesion and the surrounding cirrhotic liver. Moderately or poorly differentiated HCCs show large differences in the number of Kupffer cells compared with the surrounding cirrhotic liver and thus demonstrate a high CNR at SPIO-enhanced MRI. Dysplastic nodules and most well-differentiated HCCs, on the other hand, contain nearly the same number of Kupffer cells as the surrounding cirrhotic hepatic parenchyma and therefore are not well depicted on T2w MRI[103], although in some cases of well-differentiated HCC there can be decreased uptake of SPIO particles[94].

Some authors have proposed the possibility of a single-visit sequential SPIO-Gd protocol to obtain better diagnostic confidence[104]. Ward *et al*[105] found that the combination of Gd and ferumoxides in double-contrast MRI, compared with ferumoxides-enhanced imaging alone, led to an improvement in the diagnosis of HCC, especially for small (< 1 cm) lesions, for which the sensitivity for detection increased from 14% to 46%, compared with larger lesions (1 cm or larger), for which the sensitivity increased from 81% to 91% with the

addition of Gd-enhanced imaging. Gd-enhanced images obtained during the arterial and portal venous phases of enhancement were essential for differentiating HCC from adjacent fibrosis, which is the most frequent cause of false-positive findings of SPIO-enhanced and SPIO-unenhanced images.

Pauleit *et al*[106] found that for detection of small HCCs, the sensitivity and accuracy with unenhanced and Gd-enhanced imaging were significantly ($P = 0.017$) superior to those with unenhanced and ferumoxides-enhanced imaging, whereas for large HCCs the ferumoxides set was superior to the Gd set, although this difference was not statistically significant. Analysis of all HCCs revealed no significant differences for Gd-enhanced and ferumoxides-enhanced imaging[106].

### *Fibrolamellar HCC (FL-HCC)*

FL-HCC is a distinctive type of HCC that occurs in younger patients (mean age 20 years)[96]. Although it is a malignant lesion, the prognosis is better than that of typical HCC, with 25% of patients having resectable lesions. α-fetoprotein levels are usually not elevated. FL-HCC is typically a well-circumscribed lesion that is hypo-intense on T1w images and hyperintense on T2w images[96]. A central scar may be present. Central calcifications are present in one third of lesions. The differential diagnosis includes mainly FNH.

To our knowledge, there are no reports of FL-HCC enhancement patterns after SPIO. Such lesions would not be expected to enhance significantly.

### *Cholangiocellular carcinoma (CCC)*

CCC is a malignant hepatic tumor of the biliary epithelium and is the second most common form of primary hepatic malignancy in adults after HCC[107]. It represents less than 1% of all newly diagnosed cancers in North America and is usually seen in the seventh decade of life[108].

Several factors have been linked etiologically to the development of CCC, although none of the factors is evident in many patients. CCC is associated with clonorchiasis, intrahepatic stone disease, choledochal cyst, Caroli disease, and primary sclerosing cholangitis (PSC)[109]. Most of these risk factors have in common long-standing inflammation and injury to the bile duct epithelium. PSC is commonly associated with CCC, with as many as 10% of patients with PSC going on to develop CCC[109].

Microscopically the tumor is an adenocarcinoma with a glandular appearance and cells resembling biliary epithelium. Mucin and calcification sometimes can be demonstrated. A large desmoplastic reaction is typical of CCC. Mixed hepato-cholangiocellular carcinomas have been described[110]. Cholangiocarcinoma usually is divided into "intrahepatic" and "extrahepatic", depending on the site of origin. For the purposes of this discussion only the intrahepatic subgroup and the Klatskin tumors are presented:

**Intrahepatic ("peripheral") cholangiocarcinoma (ICC):** ICC is a malignant neoplasm arising from the epithelium of the intrahepatic bile ducts and represents 10% of all CCC. Hilar (Klatskin) and bile duct CCCs account for the remaining 90%[107]. This neoplasm usually is a large firm mass. In 10%-20% of cases, there are several satellite nodules around the main mass. On cut section, it is characterized by the presence of large amounts of whitish fibrous tissue. A variable amount of central necrosis could be present within the tumor, especially if it is large. Hemorrhage is rare[107].

**Klatskin ("perihilar") tumor:** The Klatskin ("perihilar") tumor is a small stricturing CCC arising at the junction of the left and right hepatic ducts. These lesions produce bilobar biliary duct obstruction and are nearly always unresectable.

On MRI, ICC has a non-specific appearance. On T2w images, the signal intensity of the tumor ranges from markedly increased to moderately increased, relative to the liver. Tumors with high fibrous content tend to have lower signal intensity on T2w images[107,111]. It is iso-intense to hypo-intense on unenhanced T1w images. The most prominent feature with central CCC on MRI is usually intrahepatic biliary duct dilatation. Morphologic changes may occur late in the disease process, with atrophy of the left lobe of the liver compared with the right lobe. The left-sided hepatic ducts may be more dilated than are those in the right lobe[96]. Vascular invasion and portal nodes should be carefully searched for because these findings preclude resection of the tumor[96].

With serial dynamic ECF-Gd enhanced images, CCCs show minimal or moderate incomplete rim of enhancement at the tumor periphery on early images, with progressive central contrast-enhancement on later images[112]. Contrast-enhancement may be better seen on delayed images because of the fibrous nature of the tumor[113].

DCE imaging with Gd-BOPTA is similar to non-specific vasculo-interstitial Gd-based contrast agents, but in the hepato-biliary phase, the lesion shows contrast-enhancement in the fibrotic area. The degree of enhancement depends on the type of CCC. Greater peripheral enhancement is noted in the early phases in large CCC, whereas greater delayed enhancement is noted in the fibrous core of the "scirrhous" CCCs in the hepatobiliary phase[64]. Occasionally some small peripheral CCCs with a large number of tumor cells and few interstitial fibrous tissues at DCE MRI images reveal strong enhancement of the whole tumor on the early phase[111]. Prolonged enhancement of the tumor on the late venous and delayed phases could be of diagnostic value[114,115].

The hepatobiliary phase after liver-specific contrast agent adds useful information for identification of small satellite lesions. Analogously, after SPIO administration,

because of the absence of Kupffer cells within the lesion, no significant uptake is observed, and there is an increase of liver-to-lesion CNR on T2w images[116].

### Liver abscess

Liver abscesses can mimic necrotic liver metastases. DWI might aid in the differentiation between purulent abscesses and necrotic metastases. However, in many cases, drainage is needed for diagnostic and therapeutic purposes.

### Angiomyolipoma (AML)

AMLs are mesenchymal tumors composed of varying proportions of blood vessels, smooth muscle and mature adipose tissue. These tumors are common in the kidneys, but hepatic AMLs are very rare[117]. As these lesions are benign, preoperative diagnosis would obviate unnecessary surgery.

In patients with tuberous sclerosis, hepatic AMLs are typically small and multiple and show imaging features consistent with fat on imaging. Contrary to the imaging appearances of hepatic AMLs in patients with tuberous sclerosis, sporadic hepatic AMLs have a varied appearance because of the inconstant proportion of fat, making confident imaging diagnosis difficult and necessitating biopsy in many cases[117]. Sporadic AMLs appear to be radiologically heterogeneous, reflecting the variable proportions of fat, smooth muscle and blood vessels. In contrast to patients with tuberous sclerosis, most sporadic AMLs are solitary. Depending on the components of the sporadic AML, imaging usually shows a hypervascular tumor with heterogeneous areas of fat. In-and-out-of-phase imaging (chemical shift imaging) is useful for the detection of the fatty tissue within AMLs. Contrast-enhanced MRI can be useful to better depict the presence of vessels within AMLs. The presence of fat combined with the presence of (especially central) vessels often is useful for the definite diagnosis of AML. Still, lipid-poor hepatic, sporadic, AML can pose a diagnostic challenge, often requiring biopsy[117].

## CONCLUSION

Although the primary modalities for liver imaging are US and CT, recent studies have suggested that CE-MRI is the most sensitive method for detecting small focal liver lesions in particular. One of the advantages of MRI in liver imaging is the better soft tissue contrast, which allows better detection and characterization of benign and malignant focal liver lesions. The development of liver-specific MRI contrast agents has further improved the diagnostic yield of MRI in lesion detection and characterization.

In addition, 2 recent developments in MRI sequences for the upper abdomen comprise unenhanced DWI and keyhole-based DCE MRI (4D THRIVE). Unenhanced DWI has been shown to allow an improved detection (b = 10 s/mm$^{2)}$ of, in particular, small (< 10 mm) focal liver lesions compared with other, more routinely used, MRI sequences and is useful as a road map sequence at the start of each MRI examination of the liver. Also, using higher b-values, the calculation of ADC value, the true diffusion coefficient, D, and the perfusion fraction, f, can be useful for the characterization of focal liver lesions. DCE 4D THRIVE enables MRI of the liver with high temporal and spatial resolution with full liver coverage. 4D THRIVE improves detection and characterization of focal liver lesions providing multiple arterial and venous phases. The characterization of focal liver lesions using parametric maps appears to be promising for differentiating benign and malignant focal liver lesions.

## REFERENCES


1 **Lodge JP.** Modern surgery for liver metastases. *Cancer Imaging* 2000; **1**: 77-85
2 **Kuszyk BS**, Bluemke DA, Urban BA, Choti MA, Hruban RH, Sitzmann JV, Fishman EK. Portal-phase contrast-enhanced helical CT for the detection of malignant hepatic tumors: sensitivity based on comparison with intraoperative and pathologic findings. *AJR Am J Roentgenol* 1996; **166**: 91-95
3 **Valls C**, Lopez E, Gumà A, Gil M, Sanchez A, Andía E, Serra J, Moreno V, Figueras J. Helical CT versus CT arterial portography in the detection of hepatic metastasis of colorectal carcinoma. *AJR Am J Roentgenol* 1998; **170**: 1341-1347
4 **Ward J**, Naik KS, Guthrie JA, Wilson D, Robinson PJ. Hepatic lesion detection: comparison of MR imaging after the administration of superparamagnetic iron oxide with dual-phase CT by using alternative-free response receiver operating characteristic analysis. *Radiology* 1999; **210**: 459-466
5 **Valls C**, Andía E, Sánchez A, Gumà A, Figueras J, Torras J, Serrano T. Hepatic metastases from colorectal cancer: preoperative detection and assessment of resectability with helical CT. *Radiology* 2001; **218**: 55-60
6 **Furuhata T**, Okita K, Tsuruma T, Hata F, Kimura Y, Katsuramaki T, Mukaiya M, Hirokawa N, Ichimura T, Yama N, Koito K, Sasaki K, Hirata K. Efficacy of SPIO-MR imaging in the diagnosis of liver metastases from colorectal carcinomas. *Dig Surg* 2003; **20**: 321-325
7 **Wang SS**, Chiang JH, Tsai YT, Lee SD, Lin HC, Chou YH, Lee FY, Wang JS, Lo KJ. Focal hepatic fatty infiltration as a cause of pseudotumors: ultrasonographic patterns and clinical differentiation. *J Clin Ultrasound* 1990; **18**: 401-409
8 **Janica JR**, Lebkowska U, Ustymowicz A, Augustynowicz A, Kamocki Z, Werel D, Polaków J, Kedra B, Pepinski W. Contrast-enhanced ultrasonography in diagnosing liver metastases. *Med Sci Monit* 2007; **13** Suppl 1: 111-115
9 **Della Vigna P**, Cernigliaro F, Monfardini L, Gandini S, Bellomi M. Contrast-enhanced ultrasonography in the follow-up of patients with hepatic metastases from breast carcinoma. *Radiol Med* 2007; **112**: 47-55
10 **Dai Y**, Chen MH, Yin SS, Yan K, Fan ZH, Wu W, Wang YB, Yang W. Focal liver lesions: can SonoVue-enhanced ultrasound be used to differentiate malignant from benign lesions? *Invest Radiol* 2007; **42**: 596-603
11 **Soye JA**, Mullan CP, Porter S, Beattie H, Barltrop AH, Nelson WM. The use of contrast-enhanced ultrasound in the characterisation of focal liver lesions. *Ulster Med J* 2007; **76**: 22-25
12 **Rappeport ED**, Loft A. Liver metastases from colorectal

cancer: imaging with superparamagnetic iron oxide (SPIO)-enhanced MR imaging, computed tomography and positron emission tomography. *Abdom Imaging* 2007; **32**: 624-634
13 **Silverman PM**. Liver metastases: imaging considerations for protocol development with multislice CT (MSCT). *Cancer Imaging* 2006; **6**: 175-181
14 **Wiering B**, Ruers TJ, Krabbe PF, Dekker HM, Oyen WJ. Comparison of multiphase CT, FDG-PET and intra-operative ultrasound in patients with colorectal liver metastases selected for surgery. *Ann Surg Oncol* 2007; **14**: 818-826
15 **Morana G**, Salviato E, Guarise A. Contrast agents for hepatic MRI. *Cancer Imaging* 2007; **7** Spec No A: S24-S27
16 **Zech CJ**, Grazioli L, Jonas E, Ekman M, Niebecker R, Gschwend S, Breuer J, Jönsson L, Kienbaum S. Health-economic evaluation of three imaging strategies in patients with suspected colorectal liver metastases: Gd-EOB-DTPA-enhanced MRI vs. extracellular contrast media-enhanced MRI and 3-phase MDCT in Germany, Italy and Sweden. *Eur Radiol* 2009; **19** Suppl 3: S753-S763
17 **Semelka RC**, Cance WG, Marcos HB, Mauro MA. Liver metastases: comparison of current MR techniques and spiral CT during arterial portography for detection in 20 surgically staged cases. *Radiology* 1999; **213**: 86-91
18 **Hagspiel KD**, Neidl KF, Eichenberger AC, Weder W, Marincek B. Detection of liver metastases: comparison of superparamagnetic iron oxide-enhanced and unenhanced MR imaging at 1.5 T with dynamic CT, intraoperative US, and percutaneous US. *Radiology* 1995; **196**: 471-478
19 **Senéterre E**, Taourel P, Bouvier Y, Pradel J, Van Beers B, Daures JP, Pringot J, Mathieu D, Bruel JM. Detection of hepatic metastases: ferumoxides-enhanced MR imaging versus unenhanced MR imaging and CT during arterial portography. *Radiology* 1996; **200**: 785-792
20 **Müller RD**, Vogel K, Neumann K, Hirche H, Barkhausen J, Stöblen F, Henrich H, Langer R. SPIO-MR imaging versus double-phase spiral CT in detecting malignant lesions of the liver. *Acta Radiol* 1999; **40**: 628-635
21 **Lencioni R**, Della Pina C, Bruix J, Majno P, Grazioli L, Morana G, Filippone A, Laghi A, Bartolozzi C. Clinical management of hepatic malignancies: ferucarbotran-enhanced magnetic resonance imaging versus contrast-enhanced spiral computed tomography. *Dig Dis Sci* 2005; **50**: 533-537
22 **Ward J**. New MR techniques for the detection of liver metastases. *Cancer Imaging* 2006; **6**: 33-42
23 **Kim YK**, Lee JM, Kim CS, Chung GH, Kim CY, Kim IH. Detection of liver metastases: gadobenate dimeglumine-enhanced three-dimensional dynamic phases and one-hour delayed phase MR imaging versus superparamagnetic iron oxide-enhanced MR imaging. *Eur Radiol* 2005; **15**: 220-228
24 **Kim MJ**, Kim JH, Lim JS, Oh YT, Chung JJ, Choi JS, Lee WJ, Kim KW. Detection and characterization of focal hepatic lesions: mangafodipir vs. superparamagnetic iron oxide-enhanced magnetic resonance imaging. *J Magn Reson Imaging* 2004; **20**: 612-621
25 **Le Bihan D**, Breton E, Lallemand D, Aubin ML, Vignaud J, Laval-Jeantet M. Separation of diffusion and perfusion in intravoxel incoherent motion MR imaging. *Radiology* 1988; **168**: 497-505
26 **Yamada I**, Aung W, Himeno Y, Nakagawa T, Shibuya H. Diffusion coefficients in abdominal organs and hepatic lesions: evaluation with intravoxel incoherent motion echo-planar MR imaging. *Radiology* 1999; **210**: 617-623
27 **Coenegrachts K**, Delanote J, Ter Beek L, Haspeslagh M, Bipat S, Stoker J, Steyaert L, Rigauts H. Evaluation of true diffusion, perfusion factor, and apparent diffusion coefficient in non-necrotic liver metastases and uncomplicated liver hemangiomas using black-blood echo planar imaging. *Eur J Radiol* 2009; **69**: 131-138
28 **Nagayama M**, Watanabe Y, Okumura A, Tabuchi T, Mitsui H, Morimoto N, Nakada K, Kumashiro M, Kiyono Y, Amoh Y, Nakashita S, Dodo Y, Geraats D, Van Cauteren M. Black-blood T2-weighted SE-EPI Imaging of the Liver. *Proc Intl SOC Mag Reson Med* 2002; **10**: 1963
29 **Coenegrachts K**, Orlent H, ter Beek L, Haspeslagh M, Bipat S, Stoker J, Rigauts H. Improved focal liver lesion detection: comparison of single-shot spin-echo echo-planar and superparamagnetic iron oxide (SPIO)-enhanced MRI. *J Magn Reson Imaging* 2008; **27**: 117-124
30 **Coenegrachts K**, De Geeter F, ter Beek L, Walgraeve N, Bipat S, Stoker J, Rigauts H. Comparison of MRI (including SS SE-EPI and SPIO-enhanced MRI) and FDG-PET/CT for the detection of colorectal liver metastases. *Eur Radiol* 2009; **19**: 370-379
31 **Hussain SM**, De Becker J, Hop WC, Dwarkasing S, Wielopolski PA. Can a single-shot black-blood T2-weighted spin-echo echo-planar imaging sequence with sensitivity encoding replace the respiratory-triggered turbo spin-echo sequence for the liver? An optimization and feasibility study. *J Magn Reson Imaging* 2005; **21**: 219-229
32 **Nasu K**, Kuroki Y, Nawano S, Kuroki S, Tsukamoto T, Yamamoto S, Motoori K, Ueda T. Hepatic metastases: diffusion-weighted sensitivity-encoding versus SPIO-enhanced MR imaging. *Radiology* 2006; **239**: 122-130
33 **Sun XJ**, Quan XY, Huang FH, Xu YK. Quantitative evaluation of diffusion-weighted magnetic resonance imaging of focal hepatic lesions. *World J Gastroenterol* 2005; **11**: 6535-6537
34 **Koh DM**, Erica S, Collins D, Reinsberg S, Brown G, Leach M, Cunningham D, Husband J. Diffusion coefficients and the perfusion fraction of colorectal hepatic metastases estimated using single-shot echo-planar sensitivity-encoded (SENSE) diffusion-weighted MR imaging. *Proc Intl Soc Mag Reson Med* 2004; **11**: 908
35 **Low RN**. Abdominal MRI advances in the detection of liver tumours and characterisation. *Lancet Oncol* 2007; **8**: 525-535
36 **Rofsky NM**, Lee VS, Laub G, Pollack MA, Krinsky GA, Thomasson D, Ambrosino MM, Weinreb JC. Abdominal MR imaging with a volumetric interpolated breath-hold examination. *Radiology* 1999; **212**: 876-884
37 **Bonaldi VM,** Bret PM, Reinhold C, Atri M. Helical CT of the liver: value of an early hepatic arterial phase. *Radiology* 1995; **197**: 357-363
38 **Lee VS**, Lavelle MT, Rofsky NM, Laub G, Thomasson DM, Krinsky GA, Weinreb JC. Hepatic MR imaging with a dynamic contrast-enhanced isotropic volumetric interpolated breath-hold examination: feasibility, reproducibility, and technical quality. *Radiology* 2000; **215**: 365-372
39 **Beck GM**, De Becker J, Jones AC, von Falkenhausen M, Willinek WA, Gieseke J. Contrast-enhanced timing robust acquisition order with a preparation of the longitudinal signal component (CENTRA plus) for 3D contrast-enhanced abdominal imaging. *J Magn Reson Imaging* 2008; **27**: 1461-1467
40 **Beck G**, Herigault G, Glantenay A, Coenegrachts K, Denolin V. Ultra-fast time resolved contrast enhanced abdominal imaging using an elliptical centric fat suppressed 3D profile sharing acquisition technique, SENSE and partial Fourier. *Proc Intl Soc Mag Reson Med* 2008; **16**: 2622
41 **Coenegrachts K**, Ghekiere J, Denolin V, Gabriele B, Hérigault G, Haspeslagh M, Daled P, Bipat S, Stoker J, Rigauts H. Perfusion maps of the whole liver based on high temporal and spatial resolution contrast-enhanced MRI (4D THRIVE): Feasibility and initial results in focal liver lesions. *Eur J Radiol* 2009; Epub ahead of print
42 **Padhani AR**. MRI for assessing antivascular cancer treatments. *Br J Radiol* 2003; **76** Spec No 1: S60-S80

43 **Wang L**, Van den Bos IC, Hussain SM, Pattynama PM, Vogel MW, Krestin GP. Post-processing of dynamic gadolinium-enhanced magnetic resonance imaging exams of the liver: explanation and potential clinical applications for color-coded qualitative and quantitative analysis. *Acta Radiol* 2008; **49**: 6-18

44 **Pandharipande PV**, Krinsky GA, Rusinek H, Lee VS. Perfusion imaging of the liver: current challenges and future goals. *Radiology* 2005; **234**: 661-673

45 **Evelhoch JL.** Key factors in the acquisition of contrast kinetic data for oncology. *J Magn Reson Imaging* 1999; **10**: 254-259

46 **Kuhl CK**, Mielcareck P, Klaschik S, Leutner C, Wardelmann E, Gieseke J, Schild HH. Dynamic breast MR imaging: are signal intensity time course data useful for differential diagnosis of enhancing lesions? *Radiology* 1999; **211**: 101-110

47 **Mayr NA**, Yuh WT, Zheng J, Ehrhardt JC, Magnotta VA, Sorosky JI, Pelsang RE, Oberley LW, Hussey DH. Prediction of tumor control in patients with cervical cancer: analysis of combined volume and dynamic enhancement pattern by MR imaging. *AJR Am J Roentgenol* 1998; **170**: 177-182

48 **Hawighorst H**, Weikel W, Knapstein PG, Knopp MV, Zuna I, Schönberg SO, Vaupel P, van Kaick G. Angiogenic activity of cervical carcinoma: assessment by functional magnetic resonance imaging-based parameters and a histomorphological approach in correlation with disease outcome. *Clin Cancer Res* 1998; **4**: 2305-2312

49 **Hulka CA**, Edmister WB, Smith BL, Tan L, Sgroi DC, Campbell T, Kopans DB, Weisskoff RM. Dynamic echo-planar imaging of the breast: experience in diagnosing breast carcinoma and correlation with tumor angiogenesis. *Radiology* 1997; **205**: 837-842

50 **Lin MX**, Xu HX, Lu MD, Xie XY, Chen LD, Xu ZF, Liu GJ, Xie XH, Liang JY, Wang Z. Diagnostic performance of contrast-enhanced ultrasound for complex cystic focal liver lesions: blinded reader study. *Eur Radiol* 2009; **19**: 358-369

51 **Valls C**, Reñe M, Gil M, Sanchez A, Narvaez JA, Hidalgo F. Giant cavernous hemangioma of the liver: atypical CT and MR findings. *Eur Radiol* 1996; **6**: 448-450

52 **Vilgrain V**, Boulos L, Vullierme MP, Denys A, Terris B, Menu Y. Imaging of atypical hemangiomas of the liver with pathologic correlation. *Radiographics* 2000; **20**: 379-397

53 **Ros PR**. Benign liver lesion. In: Gore RM, Levin MS, Laufer I, editors. Textbook of Gastrointestinal Radiology. Philadelphia: WB Saunders, 1994: 1861-1896

54 **Semelka RC**, Brown ED, Ascher SM, Patt RH, Bagley AS, Li W, Edelman RR, Shoenut JP, Brown JJ. Hepatic hemangiomas: a multi-institutional study of appearance on T2-weighted and serial gadolinium-enhanced gradient-echo MR images. *Radiology* 1994; **192**: 401-406

55 **Soyer P**, Gueye C, Somveille E, Laissy JP, Scherrer A. MR diagnosis of hepatic metastases from neuroendocrine tumors versus hemangiomas: relative merits of dynamic gadolinium chelate-enhanced gradient-recalled echo and unenhanced spin-echo images. *AJR Am J Roentgenol* 1995; **165**: 1407-1413

56 **Hanafusa K**, Ohashi I, Himeno Y, Suzuki S, Shibuya H. Hepatic hemangioma: findings with two-phase CT. *Radiology* 1995; **196**: 465-469

57 **van Leeuwen MS**, Noordzij J, Feldberg MA, Hennipman AH, Doornewaard H. Focal liver lesions: characterization with triphasic spiral CT. *Radiology* 1996; **201**: 327-336

58 **Kim T**, Federle MP, Baron RL, Peterson MS, Kawamori Y. Discrimination of small hepatic hemangiomas from hypervascular malignant tumors smaller than 3 cm with three-phase helical CT. *Radiology* 2001; **219**: 699-706

59 **Grangier C**, Tourniaire J, Mentha G, Schiau R, Howarth N, Chachuat A, Grossholz M, Terrier F. Enhancement of liver hemangiomas on T1-weighted MR SE images by superparamagnetic iron oxide particles. *J Comput Assist Tomogr* 1994; **18**: 888-896

60 **Denys A**, Arrive L, Servois V, Dubray B, Najmark D, Sibert A, Menu Y. Hepatic tumors: detection and characterization at 1-T MR imaging enhanced with AMI-25. *Radiology* 1994; **193**: 665-669

61 **Kim JH**, Kim MJ, Suh SH, Chung JJ, Yoo HS, Lee JT. Characterization of focal hepatic lesions with ferumoxides-enhanced MR imaging: utility of T1-weighted spoiled gradient recalled echo images using different echo times. *J Magn Reson Imaging* 2002; **15**: 573-583

62 **Yu JS**, Kim MJ, Kim KW, Chang JC, Jo BJ, Kim TH, Lee JT, Yoo HS. Hepatic cavernous hemangioma: sonographic patterns and speed of contrast enhancement on multiphase dynamic MR imaging. *AJR Am J Roentgenol* 1998; **171**: 1021-1025

63 **Whitney WS**, Herfkens RJ, Jeffrey RB, McDonnell CH, Li KC, Van Dalsem WJ, Low RN, Francis IR, Dabatin JF, Glazer GM. Dynamic breath-hold multiplanar spoiled gradient-recalled MR imaging with gadolinium enhancement for differentiating hepatic hemangiomas from malignancies at 1.5 T. *Radiology* 1993; **189**: 863-870

64 **Petersein J**, Spinazzi A, Giovagnoni A, Soyer P, Terrier F, Lencioni R, Bartolozzi C, Grazioli L, Chiesa A, Manfredi R, Marano P, Van Persijn Van Meerten EL, Bloem JL, Petre C, Marchal G, Greco A, McNamara MT, Heuck A, Reiser M, Laniado M, Claussen C, Daldrup HE, Rummeny E, Kirchin MA, Pirovano G, Hamm B. Focal liver lesions: evaluation of the efficacy of gadobenate dimeglumine in MR imaging--a multicenter phase III clinical study. *Radiology* 2000; **215**: 727-736

65 **Oudkerk M**, Torres CG, Song B, König M, Grimm J, Fernandez-Cuadrado J, Op de Beeck B, Marquardt M, van Dijk P, de Groot JC. Characterization of liver lesions with mangafodipir trisodium-enhanced MR imaging: multicenter study comparing MR and dual-phase spiral CT. *Radiology* 2002; **223**: 517-524

66 **Ferrucci JT**. Liver tumor imaging. Current concepts. *Radiol Clin North Am* 1994; **32**: 39-54

67 **Fong Y**, Blumgart LH, Fortner JG, Brennan MF. Pancreatic or liver resection for malignancy is safe and effective for the elderly. *Ann Surg* 1995; **222**: 426-434; discussion 434-437

68 **Wernecke K**, Rummeny E, Bongartz G, Vassallo P, Kivelitz D, Wiesmann W, Peters PE, Reers B, Reiser M, Pircher W. Detection of hepatic masses in patients with carcinoma: comparative sensitivities of sonography, CT, and MR imaging. *AJR Am J Roentgenol* 1991; **157**: 731-739

69 **Schulz W**, Borchard F. [The size of the liver metastases in a low metastatic count. A quantitative study of postmortem livers] *Rofo* 1992; **156**: 320-324

70 **Imam K**, Bluemke DA. MR imaging in the evaluation of hepatic metastases. *Magn Reson Imaging Clin N Am* 2000; **8**: 741-756

71 **Outwater E**, Tomaszewski JE, Daly JM, Kressel HY. Hepatic colorectal metastases: correlation of MR imaging and pathologic appearance. *Radiology* 1991; **180**: 327-332

72 **Semelka RC**, Bagley AS, Brown ED, Kroeker MA. Malignant lesions of the liver identified on T1- but not T2-weighted MR images at 1.5 T. *J Magn Reson Imaging* 1994; **4**: 315-318

73 **Semelka RC**, Kelekis NL. Liver. In: Semelka RC, Ascher SM, Reinhold C, editors. MRI of the abdomen and pelvis: a text-atlas. New York: Wiley-Liss, 1997; 19-135

74 **Morana G**, Grazioli L, Testoni M, Caccia P, Procacci C. Contrast agents for hepatic magnetic resonance imaging. *Top Magn Reson Imaging* 2002; **13**: 117-150

75 **Oudkerk M**, van den Heuvel AG, Wielopolski PA, Schmitz PI, Borel Rinkes IH, Wiggers T. Hepatic lesions: detection with ferumoxide-enhanced T1-weighted MR imaging.

*Radiology* 1997; **203**: 449-456
76 **Larson RE**, Semelka RC, Bagley AS, Molina PL, Brown ED, Lee JK. Hypervascular malignant liver lesions: comparison of various MR imaging pulse sequences and dynamic CT. *Radiology* 1994; **192**: 393-399
77 **Benhamou JP**. [Oral contraceptives and benign tumors of the liver] *Gastsroenterol Clin Biol* 1997; **21**: 913-915
78 **Grazioli L**, Morana G, Kirchin MA, Caccia P, Romanini L, Bondioni MP, Procacci C, Chiesa A. MRI of focal nodular hyperplasia (FNH) with gadobenate dimeglumine (Gd-BOPTA) and SPIO (ferumoxides): an intra-individual comparison. *J Magn Reson Imaging* 2003; **17**: 593-602
79 **Grazioli L**, Morana G, Federle MP, Brancatelli G, Testoni M, Kirchin MA, Menni K, Olivetti L, Nicoli N, Procacci C. Focal nodular hyperplasia: morphologic and functional information from MR imaging with gadobenate dimeglumine. *Radiology* 2001; **221**: 731-739
80 **Leese T**, Farges O, Bismuth H. Liver cell adenomas. A 12-year surgical experience from a specialist hepato-biliary unit. *Ann Surg* 1988; **208**: 558-564
81 **Boulahdour H**, Cherqui D, Charlotte F, Rahmouni A, Dhumeaux D, Zafrani ES, Meignan M. The hot spot hepatobiliary scan in focal nodular hyperplasia. *J Nucl Med* 1993; **34**: 2105-2110
82 **Paley MR**, Mergo PJ, Torres GM, Ros PR. Characterization of focal hepatic lesions with ferumoxides-enhanced T2-weighted MR imaging. *AJR Am J Roentgenol* 2000; **175**: 159-163
83 **Grandin C**, Van Beers BE, Robert A, Gigot JF, Geubel A, Pringot J. Benign hepatocellular tumors: MRI after superparamagnetic iron oxide administration. *J Comput Assist Tomogr* 1995; **19**: 412-418
84 **Attal P**, Vilgrain V, Brancatelli G, Paradis V, Terris B, Belghiti J, Taouli B, Menu Y. Telangiectatic focal nodular hyperplasia: US, CT, and MR imaging findings with histopathologic correlation in 13 cases. *Radiology* 2003; **228**: 465-472
85 **Carlson SK**, Johnson CD, Bender CE, Welch TJ. CT of focal nodular hyperplasia of the liver. *AJR Am J Roentgenol* 2000; **174**: 705-712
86 **Vilgrain V**, Fléjou JF, Arrivé L, Belghiti J, Najmark D, Menu Y, Zins M, Vullierme MP, Nahum H. Focal nodular hyperplasia of the liver: MR imaging and pathologic correlation in 37 patients. *Radiology* 1992; **184**: 699-703
87 **Lee MJ**, Saini S, Hamm B, Taupitz M, Hahn PF, Seneterre E, Ferrucci JT. Focal nodular hyperplasia of the liver: MR findings in 35 proved cases. *AJR Am J Roentgenol* 1991; **156**: 317-320
88 **Mathieu D**, Paret M, Mahfouz AE, Caseiro-Alves F, Tran Van Nhieu J, Anglade MC, Rahmouni A, Vasile N. Hyperintense benign liver lesions on spin-echo T1-weighted MR images: pathologic correlations. *Abdom Imaging* 1997; **22**: 410-417
89 **Kier R**, Rosenfield AT. Focal nodular hyperplasia of the liver on delayed enhanced CT. *AJR Am J Roentgenol* 1989; **153**: 885-886
90 **Rubin RA**, Lichtenstein GR. Hepatic scintigraphy in the evaluation of solitary solid liver masses. *J Nucl Med* 1993; **34**: 697-705
91 **Bruix J**, Sherman M, Llovet JM, Beaugrand M, Lencioni R, Burroughs AK, Christensen E, Pagliaro L, Colombo M, Rodés J. Clinical management of hepatocellular carcinoma. Conclusions of the Barcelona-2000 EASL conference. European Association for the Study of the Liver. *J Hepatol* 2001; **35**: 421-430
92 **Ince N**, Wands JR. The increasing incidence of hepatocellular carcinoma. *N Engl J Med* 1999; **340**: 798-799
93 **Zaman SN**, Melia WM, Johnson RD, Portmann BC, Johnson PJ, Williams R. Risk factors in development of hepatocellular carcinoma in cirrhosis: prospective study of 613 patients. *Lancet* 1985; **1**: 1357-1360
94 **Kudo M**. Multistep human hepatocarcinogenesis: correlation of imaging with pathology. *J Gastroenterol* 2009; **44** Suppl 19: 112-118
95 **Ishizaki M**, Ashida K, Higashi T, Nakatsukasa H, Kaneyoshi T, Fujiwara K, Nouso K, Kobayashi Y, Uemura M, Nakamura S, Tsuji T. The formation of capsule and septum in human hepatocellular carcinoma. *Virchows Arch* 2001; **438**: 574-580
96 **Kamel IR**, Bluemke DA. MR imaging of liver tumors. *Radiol Clin North Am* 2003; **41**: 51-65
97 **Forner A**, Vilana R, Ayuso C, Bianchi L, Solé M, Ayuso JR, Boix L, Sala M, Varela M, Llovet JM, Brú C, Bruix J. Diagnosis of hepatic nodules 20 mm or smaller in cirrhosis: Prospective validation of the noninvasive diagnostic criteria for hepatocellular carcinoma. *Hepatology* 2008; **47**: 97-104
98 **Krinsky GA**, Lee VS, Theise ND, Weinreb JC, Rofsky NM, Diflo T, Teperman LW. Hepatocellular carcinoma and dysplastic nodules in patients with cirrhosis: prospective diagnosis with MR imaging and explantation correlation. *Radiology* 2001; **219**: 445-454
99 **Vandecaveye V**, De Keyzer F, Verslype C, Op de Beeck K, Komuta M, Topal B, Roebben I, Bielen D, Roskams T, Nevens F, Dymarkowski S. Diffusion-weighted MRI provides additional value to conventional dynamic contrast-enhanced MRI for detection of hepatocellular carcinoma. *Eur Radiol* 2009; **19**: 2456-2466
100 **Earls JP**, Rofsky NM, DeCorato DR, Krinsky GA, Weinreb JC. Hepatic arterial-phase dynamic gadolinium-enhanced MR imaging: optimization with a test examination and a power injector. *Radiology* 1997; **202**: 268-273
101 **Frederick MG**, McElaney BL, Singer A, Park KS, Paulson EK, McGee SG, Nelson RC. Timing of parenchymal enhancement on dual-phase dynamic helical CT of the liver: how long does the hepatic arterial phase predominate? *AJR Am J Roentgenol* 1996; **166**: 1305-1310
102 **Yu JS**, Kim KW, Kim EK, Lee JT, Yoo HS. Contrast enhancement of small hepatocellular carcinoma: usefulness of three successive early image acquisitions during multiphase dynamic MR imaging. *AJR Am J Roentgenol* 1999; **173**: 597-604
103 **Lim JH**, Choi D, Cho SK, Kim SH, Lee WJ, Lim HK, Park CK, Paik SW, Kim YI. Conspicuity of hepatocellular nodular lesions in cirrhotic livers at ferumoxides-enhanced MR imaging: importance of Kupffer cell number. *Radiology* 2001; **220**: 669-676
104 **Kubaska S**, Sahani DV, Saini S, Hahn PF, Halpern E. Dual contrast enhanced magnetic resonance imaging of the liver with superparamagnetic iron oxide followed by gadolinium for lesion detection and characterization. *Clin Radiol* 2001; **56**: 410-415
105 **Ward J**, Guthrie JA, Scott DJ, Atchley J, Wilson D, Davies MH, Wyatt JI, Robinson PJ. Hepatocellular carcinoma in the cirrhotic liver: double-contrast MR imaging for diagnosis. *Radiology* 2000; **216**: 154-162
106 **Pauleit D**, Textor J, Bachmann R, Conrad R, Flacke S, Layer G, Kreft B, Schild H. Hepatocellular carcinoma: detection with gadolinium- and ferumoxides-enhanced MR imaging of the liver. *Radiology* 2002; **222**: 73-80
107 **Craig J**, Peters R, Edmonson H. Tumors of the Liver and Intrahepatic Bile Ducts: Atlas of Tumor Pathology. Washington, DC: Armed Forced Institute of Pathology, 1989
108 **Bloom CM**, Langer B, Wilson SR. Role of US in the detection, characterization, and staging of cholangiocarcinoma. *Radiographics* 1999; **19**: 1199-1218
109 **Sherlock S**, Dooley J, editors. Diseases of the liver and biliary system. London: Blackwell Science, 1997
110 **Hashimoto T**, Nakamura H, Hori S, Tomoda K, Mitani T, Murakami T, Kozuka T, Monden M, Wakasa K, Sakurai M. MR imaging of mixed hepatocellular and cholangiocellular

carcinoma. *Abdom Imaging* 1994; **19**: 430-432
111 **Vilgrain V**, Van Beers BE, Flejou JF, Belghiti J, Delos M, Gautier AL, Zins M, Denys A, Menu Y. Intrahepatic cholangiocarcinoma: MRI and pathologic correlation in 14 patients. *J Comput Assist Tomogr* 1997; **21**: 59-65
112 **Maetani Y**, Itoh K, Watanabe C, Shibata T, Ametani F, Yamabe H, Konishi J. MR imaging of intrahepatic cholangiocarcinoma with pathologic correlation. *AJR Am J Roentgenol* 2001; **176**: 1499-1507
113 **Murakami T**, Nakamura H, Tsuda K, Ishida T, Tomoda K, Hori S, Monden M, Kanai T, Wakasa K, Sakurai M. Contrast-enhanced MR imaging of intrahepatic cholangiocarcinoma: pathologic correlation study. *J Magn Reson Imaging* 1995; **5**: 165-170
114 **Zhang Y**, Uchida M, Abe T, Nishimura H, Hayabuchi N, Nakashima Y. Intrahepatic peripheral cholangiocarcinoma: comparison of dynamic CT and dynamic MRI. *J Comput Assist Tomogr* 1999; **23**: 670-677
115 **Yoshida Y**, Imai Y, Murakami T, Nishikawa M, Kurokawa M, Yonezawa T, Tokunaga K, Fukushima Y, Wakasa K, Kim T, Nakamura H, Sakon M, Monden M. Intrahepatic cholangiocarcinoma with marked hypervascularity. *Abdom Imaging* 1999; **24**: 66-68
116 **Vogl TJ**, Hammerstingl R, Schwarz W, Kümmel S, Müller PK, Balzer T, Lauten MJ, Balzer JO, Mack MG, Schimpfky C, Schrem H, Bechstein WO, Neuhaus P, Felix R. Magnetic resonance imaging of focal liver lesions. Comparison of the superparamagnetic iron oxide resovist versus gadolinium-DTPA in the same patient. *Invest Radiol* 1996; **31**: 696-708
117 **Low SC**, Peh WC, Muttarak M, Cheung HS, Ng IO. Imaging features of hepatic angiomyolipomas. *J Med Imaging Radiat Oncol* 2008; **52**: 118-123

**S- Editor** Cheng JX **L- Editor** Cant MR **E- Editor** Zheng XM